AIAA JOURNAL
Vol. 60, No. 7, July 2022

Technical Notes

Jet-Driven Unstart Process of a Hypersonic Inlet with Ramp Mass Injection

Jiang-Jiang Li,* Hao Chen,† and Xiao-Tong Tong‡
State Key Laboratory of High Temperature Gas Dynamics, Institute of Mechanics, Chinese Academy of Sciences, 100190 Beijing, People's Republic of China
Xiong Gao§
Beijing Power Machinery Institute, 100074 Beijing, People's Republic of China
and
Qi-Fan Zhang¶ and Lian-Jie Yue**
State Key Laboratory of High Temperature Gas Dynamics, Institute of Mechanics, Chinese Academy of Sciences, 100190 Beijing, People's Republic of China

https://doi.org/10.2514/1.J061392

I. Introduction

UNSTART that arises in hypersonic inlets is a seriously threatening phenomenon for airbreathing hypersonic flight [1]. Aerodynamically, it features a massive flow separation ahead of the duct throat and a strong shock system expelled from the internal flow path. A practical outcome is the remarkable decreases in captured airflow and total pressure recovery. Due to this deficit and inferior quality of air delivery, the engine performance can be degraded significantly, which results in an abrupt thrust loss. In extreme cases, the safety of aircraft may be at stake under the influence of undesired aerodynamic and thermal loads. Given the great harm, the prevention of unstart is necessary, hence the strict requirements for inlet application. Among them is the limit of fuel addition [2].

For inlets designed for forebody-fueled scramjets [3–5], which feature better mixing rates at high Mach numbers, the restriction seems even more stringent in comparison with others. Turner and Smart [6] have observed through wall pressures that an inlet of that type suffered unstart because of an excessive combustion-induced backpressure increase once the fueling equivalence ratio exceeded 0.92 at Mach 8.1. Technically, it is not an encouraging result on tolerance because in this way the engineering practice of hypersonic engines adopting this fueling mechanism will be fairly limited, especially when an adequate margin of safety has to be left. Therefore, strategies need developing in order to improve the inlet stability. The prerequisite to this is an in-depth knowledge of the characteristics and mechanisms regarding the jet-affected unstart, which is potentially different from the commonly known and extensively studied unstart phenomenon [7] owning to the addition of jet/crossflow interactions. But unfortunately, for the severe lack of targeted research, its picture is currently quite unclear. Even worse, it appears that there has been no public report including the visualization of such an unstarted flow, and how one actually behaves is still unknown. Clearly special efforts are in demand.

In this Technical Note, a wind-tunnel study is carried out on the inlet-flow characteristics with variable ramp mass injections. Its objective is threefold: 1) to observe the flow evolution from a started inlet state to an unstarted one; 2) to explore a novel mechanism inducing unstart; 3) to provide a group of jet-involved inlet data for future computational fluid dynamics (CFD) validation. It should be noted that this study is not aimed only at forebody-fueled inlets; the results analyzed herein are also expected to facilitate the understanding of the flows in fluidically variable inlets (e.g., Ref. [8]), whose concept was developed several years ago to obtain a good low-speed performance via ramp jet.

The rest of the Note is organized as follows. The subject and methodology are firstly described. Then the experimental results are presented, along with a brief discussion on the novel unstart mechanism. Lastly, a short summary is provided.

II. Experimental Setup

A. Inlet Model

The test article is a rectangular hypersonic inlet designed for a shock-on-lip Mach number of 10.0, as shown in Fig. 1. Its capture section is 112.0 mm high and 89.6 mm wide. The ratio of area contraction is 10.0 in total, being 2.7 internally. Structurally, it consists of a ramp, a cowl, a pair of duct sidewalls, a pair of ramp-affiliated side plates, and a jet generation system. The ramp is slightly curved, having a leading inclination of 8.0 deg and a following 4 deg gradual turning ahead of the duct. The cowl is sharp-tipped and has a flat bottom surface. The duct sidewalls are designed with a swept-back angle of 54.0 deg and have two recessed windows for visualization of flow patterns inside the straight isolator, which is 11.2 mm in height and 115.0 in length. The side-plate pair forms roughly a triangular shape with a windward angle of 12.0 deg. The jet system is further composed of three subparts: two 15-mm-diam pipes for air supply, a 0.2 L air-mixing chamber, and a perforated plate flush mounted into the ramp forepart. In the plate, there are four rows of through holes perpendicular to the surface, of which the downstream three rows are not put into service in the current study. The holes in use are 1.0 mm in diameter and designed to be sonic at the exit plane. Their number is 26 and the distance away from the ramp tip is 21.0 mm.

For pressure measuring, 16 survey points are set up along the midline of ramp. They start from a position 200 mm downstream of the tip and have a horizontal spacing distance of 50.0 mm before the duct and 20.0 mm inside. On the windward side, they are small holes with a diameter of 0.8 mm and depths below 5.0 mm so that a rapid measuring response can be ensured. On the leeward side, they are threaded for easy connection to transducers. Additionally, a similar survey point is deployed in the plenum chamber to monitor the jet pressure.

B. Wind Tunnel and Measuring Apparatus

The experiments were conducted in the GJF shock tunnel, located in the Institute of Mechanics, Beijing. The facility runs in a pulsing mode, capable of generating a flow with the target Mach number for

Received 22 October 2021; revision received 16 March 2022; accepted for publication 21 March 2022; published online 7 April 2022.

*Graduate; also University of Chinese Academy of Sciences, 100049 Beijing, People's Republic of China.
†Assistant Professor; chenhao@imech.ac.cn (Corresponding Author).
‡Ph.D. Candidate; also University of Chinese Academy of Sciences, 100049 Beijing, People's Republic of China.
§Senior Engineer.
¶Assistant Professor.
**Professor.

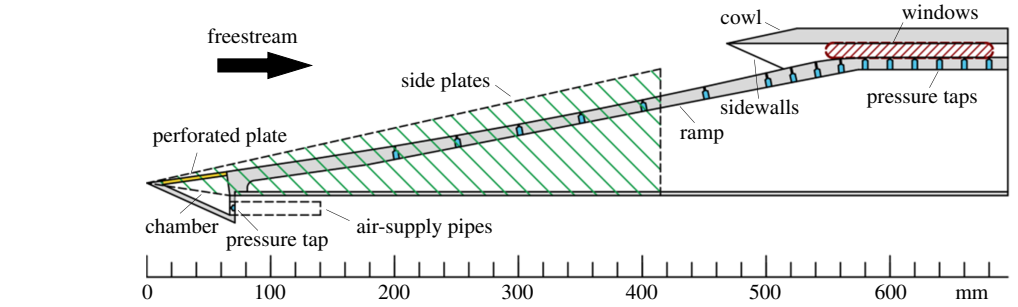

a) Sketch of the flow path

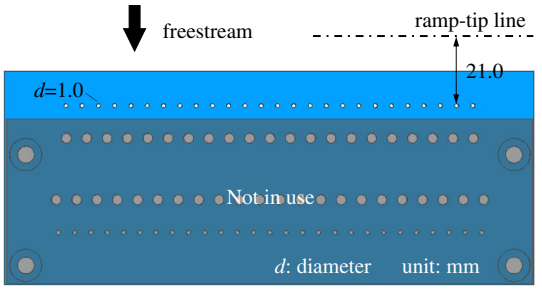

b) Perforated plate

c) Photograph of the model installed in the wind tunnel

Fig. 1 Inlet model.

15–30 ms, depending on the test condition. It has a nozzle 800 mm in diameter and can accommodate the model under investigation. Besides the main body, there is another air-supply system providing bypass jet. It contains a 1 m^3 air tank pressurized up to 4.0 MPa, a fast-response electric switch valve, a pressure-reducing valve, and auxiliary pipes. By varying the tank pressure and valve opening, the jet pressure can be controlled on demand. The experimental conditions for the current investigation are listed in Table 1.

Inlet pressures were measured by NS-2 dynamic transducers from Shanghai TM Sensor Co., Ltd. Those transducers have a measuring range of 200 kPa with an uncertainty of ±0.3% full scale. Their natural response frequencies are 30 kHz. Flow images were synchronously recorded by a high-speed schlieren system. It contains a FASTCAM SA4 camera from the Photron Ltd., which worked with a Nikkor AF-S 80–200 mm f/2.8D IF-ED lens at a frame rate of 1000 fps throughout the research. The shutter speed was 5.6 μs, and the imaging resolution is 1024 × 1024. For further information on the wind tunnel and measurements, refer to Ref. [9].

Table 1 Freestream and injection parameters

Parameter	Case A	Case B	Case C
Freestream Mach number	6.40 ± 0.02	6.40 ± 0.02	6.40 ± 0.02
Freestream stagnation pressure, $\times 10^6$ × Pa	1.69 ± 0.01	1.70 ± 0.01	1.65 ± 0.01
Freestream stagnation temperature, K	580 ± 28	580 ± 28	580 ± 28
Unit Reynolds number, $\times 10^6$ m^{-1}	9.5 ± 0.5	9.6 ± 0.5	9.3 ± 0.5
Effective runtime, ms	15	15	15
Area of injection, mm^2	0	20.4	20.4
Chamber pressure of jet, $\times 10^3$ Pa	— —	49.3 ± 0.6	56.7 ± 0.6
Ratio of chamber pressure to backpressure	— —	22.1 ± 0.3	26.4 ± 0.3
Stagnation temperature of jet, K	— —	300.0 ± 0.1	299.1 ± 0.1
Estimated ratio of jet to inlet mass flow, %	0	0.9 ± 0.01	1.0 ± 0.01

C. Numerical Validation of No-Injection Case

A three-dimensional Reynolds-averaged Navier–Stokes solver, same as the one used in Ref. [10], was adopted to supplement the mass flow rate and detailed flow pattern of case A, which is the reference of the whole study. To examine the effectiveness of the CFD code in the current study, the numerical results based on the test condition of case A are compared with the corresponding experimental data, as exhibited in Fig. 2. It shows that there is good agreement between each other, in images and in curves. Therefore, the calculated mass flow rate through the inlet, i.e., 0.27 kg/s, can be considered the actual value and utilized as a reference to compute jet-to-inlet mass flow ratios. By the way, the trial revealed a failure of this approach in predicting the jet-including cases, in contrast to the success in case A. It suggests that CFD tools intended for the research into relevant topics should be validated with specialized data; the results described below are expected to help with this work in the future.

III. Results and Discussion

When there is no injection, a seemingly plane shock is observed over the ramp to accomplish the external compression (Fig. 2a). Theoretically, there are isentropic waves following the leading shock, and the shock should be curved upward in a gradual way. But due to their weakness, those waves are hardly discernible in the image, and so is the shock curvature, especially within the experimentally visible scope. Meanwhile, the cowl shock is discovered impinging on the boundary layer developing along the ramp surface and inducing a minor separation. A separation shock and a reattachment shock are thus generated near the shoulder and reflected repeatedly in the isolator. Clearly the inlet is completely started at this stage.

The situation changes gradually if an increasing ramp injection is implemented. As the jet-inlet mass flow ratio arrives at 0.9% (case B), which is estimated on the assumption that the jet is sonic and its stagnation pressure equals the chamber pressure, the ramp shock is pushed 3.0 mm outward in comparison with the preceding case (Fig. 3). In the meantime, the internal supersonic region is totally deflected to the top wall with the duct bottom filled with subsonic air. From the pressure distributions shown in Fig. 4, where data of case A are reincorporated for clear contrast, it can be concluded for sure that

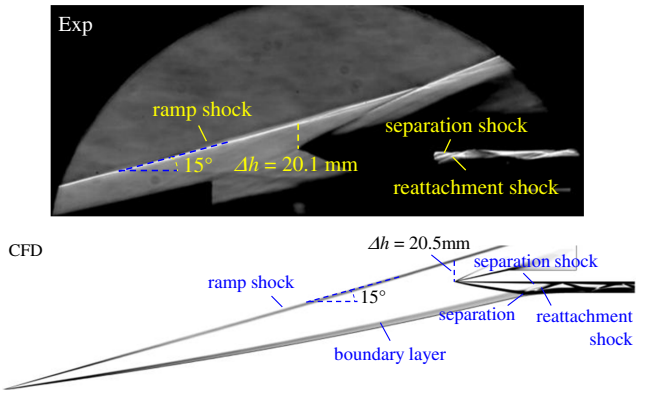

a) Schlieren images

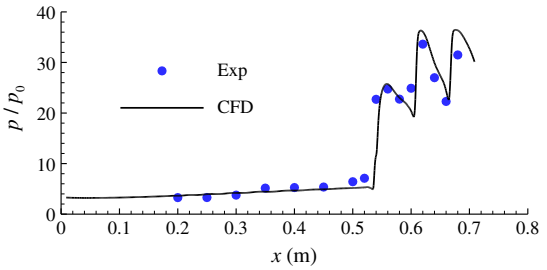

b) Surface-pressure distributions

Fig. 2 Experimental and numerical results for the case without jet (case A).

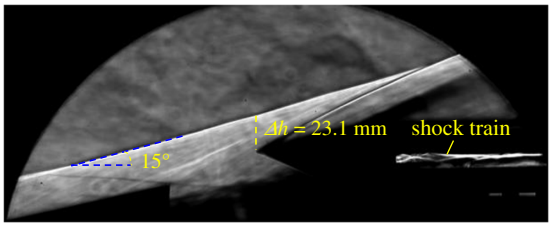

Fig. 3 Flow pattern in the case B (0.9%).

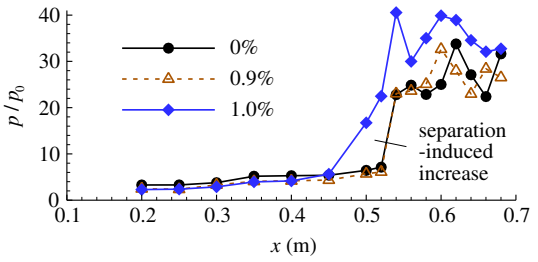

Fig. 4 Time-averaged surface-pressure distributions under different jet conditions.

flows downstream of the throat ($x = 580$ mm) are all altered. But, overall, the inlet remains started. Further slight increase in the mass injection shifts the ramp shock mildly but brings about a big transition of the downstream flow pattern (case C, Fig. 5). The most outstanding difference is the sudden emergence of a massive flow separation before the duct. That separation blocks the throat thoroughly and breaks the whole shock system previously established inside. What occurs simultaneously is the onset of inlet unsteadiness. It is observed that the separation shrinks and expands along the ramp, repeatedly and gently, which produces a type of small-amplitude flow oscillations. Regarding the category of this flow state, it is a topic meriting discussion. Generally, the criterion for distinguishing between unstart and start is whether the capture characteristic of an inlet is influenced by its internal flowfield [1]. Accordingly, in a classic two-dimensional view, the inlet flow still stays in a started regime, since no extra air spillage has arisen yet considering the location of the separation shock. However, the appearance of the large separation bubble creates a high-pressure (Fig. 4) and low-speed region upstream of the duct entrance, which inevitably provokes air leakage beside the sidewalls, as illustrated in Fig. 6. That is to say, the captured airflow is reduced owing to the great change of internal flow state, and the inlet for case C is in fact unstarted, although not very badly. The accompanying separation-dominated oscillations before the throat, which are often found in an unstarted hypersonic inlet, can be regarded as indirect evidence for this conclusion. There also is, incidentally, a flow detail of interest during the foregoing unstart process: the inclination of the ramp shock seems unaffected even if the distance from the shock to the cowl keeps increasing. It suggests that the jet-controlled ramp shock varies largely in a translational way.

Fundamentally, the observed unstart is triggered by a mechanism quite distinct from the one found by Turner and Smart [6], in which the combustion-induced choking plays the vital role. For the current case, the downstream choking has no chance to be the origin because the duct exit is fully open to the freestream all the time, instead of being throttled mechanically or thermally. This viewpoint can be further evidenced by the pressure behavior in the unstart process (Fig. 4), which shows no clear increase in the internal pressure level before the unstart and is pretty different from a downstream choking case (e.g., Fig. 4 in Ref. [11]). Relatively, a more probable explanation is that the unstart originates from the upstream jet/shock interaction and jet/boundary-layer interaction. The former is a phenomenon capable of enhancing the shock

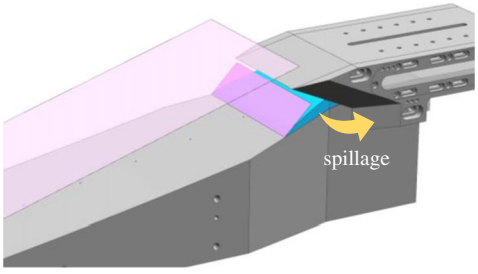

Fig. 6 Illustration of separation-induced flow spillage around the inlet.

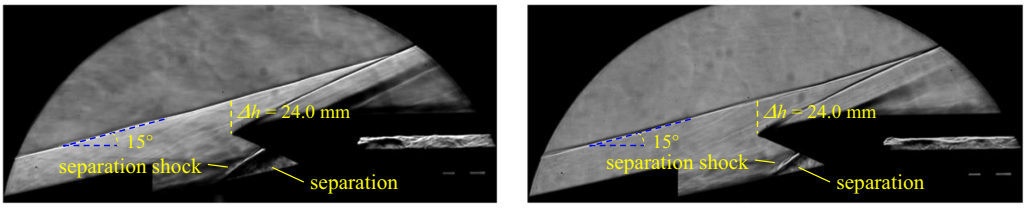

a) Largest-separation state b) Smallest-separation state

Fig. 5 Oscillating flow patterns in case C (1.0%).

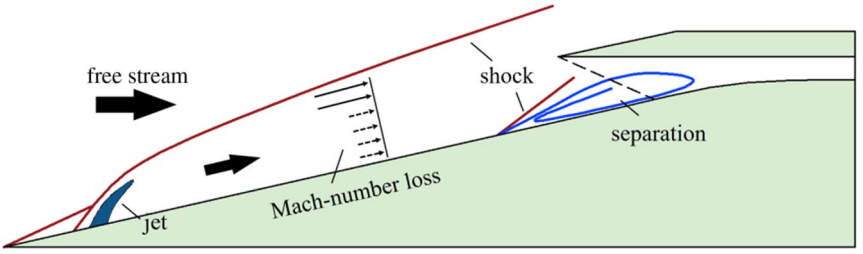

Fig. 7 Illustration of the triggering mechanism of inlet unstart.

strength locally, thereby causing an additional loss of the postshock Mach number, as shown in Fig. 7. Further, the more the jet, the lower the final Mach number. To a certain degree, it is as if an ordinary inlet faces an ever-decreasing flight Mach number. This makes the internal contraction gradually larger than the threshold allowing for flow maintenance. As for the jet/boundary-layer interaction, it can lower the momentum of the ramp boundary layer, which facilitates flow separation and thus increases the risk of unstart. Taken together, those two make it increasingly hard for the inlet to keep started as the injection rises. This is why the unstart eventually took place.

Nevertheless, despite the difference in underlying mechanism, one should notice its strong restriction on fuel addition by the same token. As far as the secondary mass flow rate alone, 1.0% of the inlet flow corresponds roughly to a limiting equivalence ratio of 0.35 for hydrogen and that of 0.14 for ethylene, which are both pretty low for practical purposes. In view of this high limit, the jet-induced unstart should be an important consideration when designing inlets and fueling strategies. However, one would worry about the generality of this phenomenon, given that the tested inlet has a swept-back sidewall design and the tested Mach number is lower than the design value. As far as we can tell, the new unstart could be a prevalent problem among inlets that employ the forebody fueling mechanism. The explanation unfolds from the following three aspects. First is the effect of side openings on jet-induced unstart. Considering that spilling air in advance is beneficial to the inlet start, the side openings are actually a factor that delays and weakens unstart. Therefore, for inlets with closed sidewalls, the unstart would be further exacerbated. The second is whether the unstart found at a lower Mach number will still be existent when the inlet operates normally. As discussed earlier, the new unstart stems from the upstream jet/crossflow interactions. Actually, it is an unstart mechanism independent of whether the inlet runs at the design point. That is to say, whatever the Mach number is, the jet tends to weaken the starting capability by interacting with the shock and boundary layer, which makes the unstart an inevitable outcome of an excessive injection. In this sense, the unstart observed herein is likely to be a general issue regardless of operating states. However, whether the threshold for unstart is still that low is uncertain. The inlet's resistance may get improved due to the increase in freestream Mach number or further lowered by enhanced jet/shock interaction, depending on the situation. But either way, the possibility of unstart should be thoroughly examined when designing and using inlets. In addition, the coupling of two unstart mechanisms (the jet-induced and the downstream choking-induced unstart) is worth noting. To isolate the upstream mass injection, we removed the factors that could cause flow choking during the experiments, leaving the inlet in a low-backpressure state. By contrast, the real situation is much worse due to the significant combustion-induced pressure increase. Predictably, the participation of high backpressure tends to shorten the unstart process, resulting in the unstart with a lower injection. In this case, it is intriguing to speculate that the unstart issue associated with the mass injection may have greater generality in practice.

In conclusion, as for forebody-fueled scramjets, inlet unstart should be carefully considered not only from the thermal aspect but also aerodynamically.

IV. Conclusions

To better understand the unstart phenomenon in forebody-fueled scramjets and provide specialized data for future CFD validation, the ramp-jet-driven unstart process of a hypersonic inlet is studied by wind-tunnel experiments. It is observed that the ramp shock shifts outward continuously with its inclination almost unchanged, as the jet-inlet mass flow ratio rises from 0 to 1.0%. Meanwhile, the internal shock system created by the cowl-shock impingement is restricted to the top half of the duct at first and then almost collapses, which is accompanied by the abrupt appearance of a large separation bubble ahead of the throat. The consequent pressure increase before the duct suggests that there is obvious air spillage around the duct and that the inlet is already unstarted, in a three-dimensional way. Unlike the previously reported unstart phenomenon induced by downstream choking, the present case is probably attributed to the upstream jet/shock interaction and jet/boundary-layer interaction. But similarly in result, it introduces a restriction on the fuel addition. It reveals that inlet unstart should be carefully considered both thermally and aerodynamically for forebody-fueled scramjets.

Acknowledgments

This work was funded in part by the National Nature Science Foundation of China (grant numbers 12102440, 11902325, and 11672309). Sincere thanks are expressed to three anonymous referees for their helpful suggestions.

References

[1] Curran, E. T., and Murthy, S. N. B. (eds.), *Scramjet Propulsion*, AIAA Education Series, AIAA, Reston, VA, 2000, pp. 447–511.

[2] Im, S., and Do, H., "Unstart Phenomena Induced by Flow Choking in Scramjet Inlet-Isolators," *Progress in Aerospace Sciences*, Vol. 97, Feb. 2018, pp. 1–21. https://doi.org/10.1016/j.paerosci.2017.12.001

[3] Alexander, D. C., Sislian, J. P., and Parent, B., "Hypervelocity Fuel/Air Mixing in Mixed-Compression Inlets of Shcramjets," *AIAA Journal*, Vol. 44, No. 10, 2006, pp. 2145–2155. https://doi.org/10.2514/1.12630

[4] Gehre, R., Wheatley, V., and Boyce, R., "Combustion Regimes in Inlet-Fueled, Low Compression Scramjets," AIAA Paper 2015-3507, 2013. https://doi.org/10.2514/6.2015-3507

[5] Sislian, J. P., and Parent, B., "Hypervelocity Fuel/Air Mixing in a Shcramjet Inlet," *Journal of Propulsion and Power*, Vol. 20, No. 2, 2004, pp. 263–272. https://doi.org/10.2514/1.9252

[6] Turner, J. C., and Smart, M. K., "Application of Inlet Injection to a Three-Dimensional Scramjet at Mach 8," *AIAA Journal*, Vol. 48, No. 4, 2010, pp. 829–838. https://doi.org/10.2514/1.J050052

[7] Chang, J. T., Li, N., Xu, K. J., Bao, W., and Yu, D. R., "Recent Research Progress on Unstart Mechanism, Detection and Control of Hypersonic Inlet," *Progress in Aerospace Sciences*, Vol. 89, Feb. 2017, pp. 1–22. https://doi.org/10.1016/j.paerosci.2016.12.001

[8] Zhang, Y., Tan, H. J., Sun, S., Chen, H., and Li, C. H., "Experimental and Numerical Investigation of a Fluidically Variable Hypersonic Inlet," *AIAA Journal*, Vol. 55, No. 8, 2017, pp. 2597–2606. https://doi.org/10.2514/1.J055767

[9] Yue, L. J., Jia, Y. N., Xu, X., Zhang, X. Y., and Zhang, P., "Effect of Cowl Shock on Restart Characteristics of Simple Ramp Type Hypersonic

Inlets with Thin Boundary Layers," *Aerospace Science and Technology*, Vol. 74, March 2018, pp. 72–80. https://doi.org/10.1016/j.ast.2017.12.018

[10] Chen, H., Tan, H. J., Zhang, Q. F., and Zhang, Y., "Throttling Process and Buzz Mechanism of a Supersonic Inlet at Overspeed Mode," *AIAA Journal*, Vol. 56, No. 5, 2018, pp. 1953–1964. https://doi.org/10.2514/1.J056674

[11] Zhang, Q. F., Tan, H. J., Sun, S., Bu, H. X., and Rao, C. Y., "Unstart of a Hypersonic Inlet with Side Compression Caused by Downstream Choking," *AIAA Journal*, Vol. 54, No. 1, 2016, pp. 28–38. https://doi.org/10.2514/1.J054095

P. Lavoie
Associate Editor